Particle and Particle Systems Characterization

Targeted Chemo-Photo Thermal Therapy: a Nanomedicine Approximation to Selective Melanoma Treatment

--Manuscript Draft--

Manuscript Number:	
Full Title:	Targeted Chemo-Photo Thermal Therapy: a Nanomedicine Approximation to Selective Melanoma Treatment
Article Type:	Full Paper
Section/Category:	
Keywords:	NAPamide, melanoma, photothermal therapy
Corresponding Author:	Maria Vallet-Regi Universidad Complutense de Madrid Madrid, SPAIN
Corresponding Author Secondary Information:	
Corresponding Author's Institution:	Universidad Complutense de Madrid
Corresponding Author's Secondary Institution:	
First Author:	Gonzalo Villaverde
First Author Secondary Information:	
Order of Authors:	Gonzalo Villaverde
	Sergio Gómez-Graña
	Eduardo Guisasola
	Isabel García
	Christoph Hanske
	Luis M. Liz-Marzán
	Alejandro Baeza
	Maria Vallet-Regi
Order of Authors Secondary Information:	
Abstract:	Melanoma is one of the most severe public health issues worldwide, not only because of the high number of cases but also for its poor prognosis in late stages. Therefore, early diagnosis and efficient treatment are key toward a future solution. However, melanoma is highly resistant to cytotoxicity in its metastatic form. In this context, we propose a therapeutic strategy based on a targeted chemo-photothermal nanotransporter for cytotoxic compounds. This approach comprises the use of core-multishell gold nanorods, coated with mesoporous silica and further covered with a thermosensitive polymer, which is vectorized for selective internalization in melanoma cells. The proposed nanoformulation is capable of releasing the transported cytotoxic compounds on demand, in response to near-IR irradiation, with high selectivity and efficacy against malignant cells, even at low concentrations, thereby providing a new tool against melanoma disease.
Additional Information:	
Question	**Response**
Please submit a plain text version of your cover letter here. Please note, if you are submitting a	Dear Editor of Particle and Particle Systems Characterization Herein you can find the revised manuscript of our work “Targeted Chemo-Photo Thermal Therapy: a Nanomedicine Approximation to Selective Melanoma Treatment.”

revision of your manuscript, there is an opportunity for you to provide your responses to the reviewers later; please do not add them to the cover letter.	(Full Paper, No. smll.201800797) This work was submitted in Small and after peer review evaluation, the editor suggested for a direct transfer in Particle and Particle Systems Characterization. The authors have taken into account all suggestions and comments made by the reviewers in the new manuscript. Here you can find a detailed response to the referees´ comments including the changes made The authors of this article thank for the effort and advice of referees and editor, who have undoubtedly contributed to enrich and improve its quality. Their reports have been taken into consideration and we have revised our manuscript in accordance with them. The answers to the referees´ queries are incorporated in our revised manuscript. Kind regards
Do you or any of your co-authors have a conflict of interest to declare?	No. The authors declare no conflict of interest.

WILEY-VCH

DOI: 10.1002/ ((please add manuscript number))
Article type: Full Paper

Targeted Chemo-Photo Thermal Therapy: a Nanomedicine Approximation to Selective Melanoma Treatment.

Gonzalo Villaverde,[a#] Sergio Gómez-Graña,[a#] Eduardo Guisasola,[a] Isabel García,[b] Christoph Hanske,[b] Luis M. Liz-Marzán,[b,c] Alejandro Baeza,[a,] Maria Vallet-Regí.[a,*]*

[a] Dpto. de Química en Ciencias Farmacéuticas, Instituto de Investigación Sanitaria Hospital, 12 de Octubre i+12.UCM. Centro de Investigación Biomédica en Red de Bioingeniería, Biomateriales y Nanomedicina (CIBER-BBN). Madrid, Spain.
[b] CIC biomaGUNE and CIBER-BBN, Paseo de Miramón 182, 20014 Donostia-San Sebastian, Spain
[c] Ikerbasque, Basque Foundation for Science, 48013 Bilbao, Spain

Keywords: NAPamide, melanoma, photothermal therapy

Abstract: Melanoma is one of the most severe public health issues worldwide, not only because of the high number of cases but also for its poor prognosis in late stages. Therefore, early diagnosis and efficient treatment are key toward a future solution. However, melanoma is highly resistant to cytotoxicity in its metastatic form. In this context, we propose a therapeutic strategy based on a targeted chemo-photothermal nanotransporter for cytotoxic compounds. This approach comprises the use of core-multishell gold nanorods, coated with mesoporous silica and further covered with a thermosensitive polymer, which is vectorized for selective internalization in melanoma cells. The proposed nanoformulation is capable of releasing the transported cytotoxic compounds on demand, in response to near-IR irradiation, with high selectivity and efficacy against malignant cells, even at low concentrations, thereby providing a new tool against melanoma disease.

1. Introduction

Melanoma is one of the most severe public health issues worldwide, as indicated by the yearly increasing number of cases.[1] Although early diagnosed melanoma is usually treated by

radical surgery, conversely, at metastatic malignant late states it has a poor prognosis.[2] Indeed, melanoma has been named as one type of tumor with the highest metastatic potential.[3] Currently, only dacarbazine as a single agent and bolus interleukin-2 as an immunotherapy alternative, have been approved by the FDA (Food and Drug Administration) as selective treatments for malignant melanoma with poor prognosis. This deficient situation has stimulated the scientific community to find novel strategies for early diagnosis and efficient treatment.

Early diagnosis is one of the keys toward reducing the risks of this malignant disease. Nowadays, the development of new synthetic strategies for radiolabeled targeting agents has afforded new diagnostic systems based on the melanoma overexpression of the melanocortin-1 receptor (MC1R). MC1R is a G-protein localized in the cell membrane, linked to skin pigmentation, which has avidity for the alpha-melanocyte stimulating hormone (α-MSH). Peptide emulations of this hormone, both linear[4] and circular[5] derivatives, named NAPamide, have been extensively used as vectorization moieties for imaging, leading to a significant improvement in early diagnosis.[6] Mechanism is based on the alpha melanocyte recognition with this receptor. MCR-1 is present in the cell wall and binds with the peptide that emulates the specific spot of interaction of the alpha melanocyte.

On the other hand, melanoma is also considered a malignant and refractory tumor in its metastatic form, highly resistant to cytotoxic agents. On account of their intrinsic and acquired properties, melanocytes have developed resistance against apoptosis. The classical treatment for most solid tumors based on the systemic administration of cytotoxic drugs, immunotherapy and cocktail combinations, usually effective against other tumors in classic chemotherapy,[7] result almost useless against melanoma.[8],[9],[10]

As a representative example, Doxorubicin (DOX) administration, because of its multiple modes of action, is one of the most relevant treatments for multiple cancerous diseases. However, melanoma is naturally resistant to its effect through the protection of the

mitochondrial DNA system[8] active in these cells, and systemic treatments result almost ineffective. Treatment with DOX, even at high doses, would only lead to an increase of multi-resistance and important side effects for the patient.

The possibility of improving the performance of DOX for the treatment of melanoma, whether metastatic or primary, has been recently studied, involving the combination of this drug with immunotherapy, vectorized conjugates and other approaches.[11],[12]

Alternatively, nanomedicine may offer promising alternatives for such extreme cases. The passive targeting, known as *Enhanced Permeability and Retention* (EPR) effect, results in nanometer-sized objects passively accumulating within tumoral mass, as a consequence of the highly porous blood vessels that irrigate the malignant tissue.[13–15] This effect has been exploited to deliver cytotoxic drugs to tumor cells in a selective manner, *via* encapsulation within nanometric carriers. In the case of DOX, previous works have reported the higher cytotoxic efficacy employing nanoformulations, as compared to classic chemotherapy in melanoma tumors.[12],[16] The increased tumor cell mortality achieved with nanocarriers can be associated with the significantly higher local concentration of DOX that can be achieved inside melanoma cells, which allows a decrease of the administered doses, thereby reducing the usually severe side effects.

On the other hand, photothermal therapy (PTT) is attracting great attention as a minimally invasive treatment for cancer therapy.[17–19] This therapy is based on the conversion of light into localized heating, mediated the strong absorption of certain nanoparticles.[20–22] This is particularly effective in the near infrared (NIR) spectral range between 650-900 nm, known as the first biological window. In this region the penetration of light in tissues is higher due to reduced absorption and scattering, which also results in marginal tissue damage.[23] Nanomaterials such as gold nanorods, gold nanoshells, gold nanocages, gold nanostars, graphene and carbon nanotubes, have been extensively studied for light-induced local heating, because of their ability to efficiently absorb NIR radiation and release it as heat.[24–27]

PPT using a NIR laser has however two main limitations: the penetration depth of the laser[28] and the amount of NIR-responsive nanoparticles that can be accumulated inside the tumor, which determines the local heating efficiency. NIR penetration depends on the specific type of tissue and the power of the irradiation source, but in any case it is limited to a few centimeters in the best cases.[29] Thus, PPT is only suitable for treatment of superficial cancers such as melanoma, uveal or even laser accessible cancers such as cervix or colon. One of the most popular types of nanocrystals for PTT are gold nanorods (GNRs).[30] GNRs have attractive optical properties related to localized surface plasmon resonances (LSPR), in particular the most intense longitudinal LSPR in the NIR, which can be tuned by the GNR dimensions, through the synthesis procedure.[31] GNRs show excellent photothermal conversion effects and generate localized hyperthermia.[21,27] The clinical application of GNRs in PTT has however been limited due to the cytotoxicity caused by the remaining surfactant cetyltrimethylammonium bromide (CTAB), which is typically used for GNR synthesis. In previous works, this problem has been solved by encapsulating the GNRs with polyethylene glycol (PEG),[32] or with mesoporous silica shells (GNR@MS).[33,34] GNR@MS nanoparticles are of particular interest, due to the properties of the mesoporous silica layer, which can not only reduce the cytotoxicity and the aggregation of GNRs, but also improve the drug-loading ability. In addition, mesoporous silica can be easily modified by introducing different functional groups, which act as anchoring points for subsequent surface modification with functional biomolecules. In Vallet-Regí's group, mesoporous silica nanoparticles have been studied as controlled drug delivery systems,[35,36] and more recently core@shell magnetite@mesoporous silica with a polymer surface coating were used as heating/stimuli-response drug delivery systems.[37] This polymeric coating exhibited a linear-to-globular transition at temperatures above 42-43 ^{o}C, thereby allowing the release of drugs encapsulated inside the mesoporous silica channels.[38]

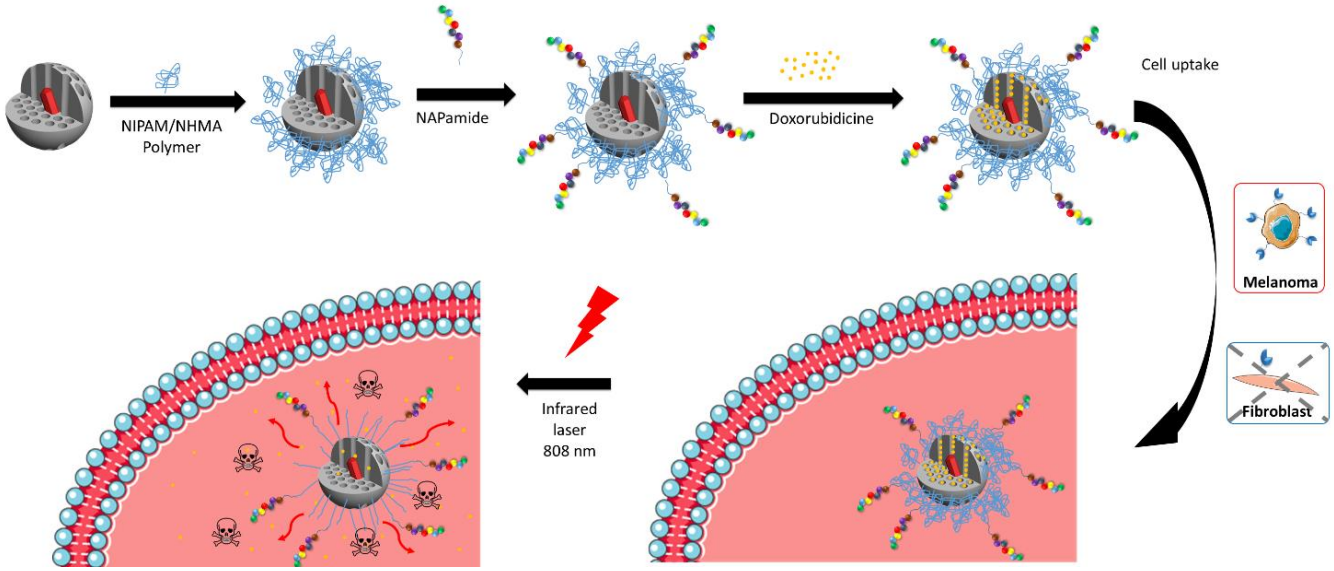

Scheme 1. Representation of a photoresponsive nanocarrier with surface anchored NAPamide targeting (PR-NC-NAP), which is proposed for melanoma treatment.

We present herein a strategy for melanoma treatment, based on core-shell GNR@MS covered with a thermosensitive polymeric shell capable of both releasing on demand the transported cytotoxic compounds, in response to NIR illumination, and selectively recognizing melanoma cells. (Scheme 1) The selectivity is provided by the external decoration of the polymer shell with NAPamide, which is expected to enhance the internalization of the drug nanocarrier inside the melanoma cancer cells, even in the presence of healthy cells. This system shows a selective capacity to destroy tumor cells by triggering drug release only when NIR light is applied, exploiting the synergic effect between the cytotoxic drug and the local temperature increase caused by the photothermal effect.[34,39,40, 41,42,43] This design provides a means to achieve a higher therapeutic efficacy while minimizing the administered drug dose.

2. Results and discussion

The first step for the construction of the "smart" nanovehicles comprised the synthesis of GNRs. To this aim, a modified seed-mediated growth method in aqueous solution was used, as described in the experimental section. **Figure 1A** shows a representative TEM micrograph of the obtained GNRs, where the monodispersity of the sample can be appreciated. The GNRs featured average length, width and aspect ratio of 43±4 nm, 10±3 nm and 3.9±0.3,

respectively. The extinction spectrum of GNRs is provided in Figure S2 (Supporting Information), displaying an intense absorbance around 808 nm due the longitudinal LSPR (λ_{max} 766 nm for bare rods, 796 after silica coating). After synthesis, GNRs were washed by centrifugation to remove excess reactants and coated with mesoporous silica.

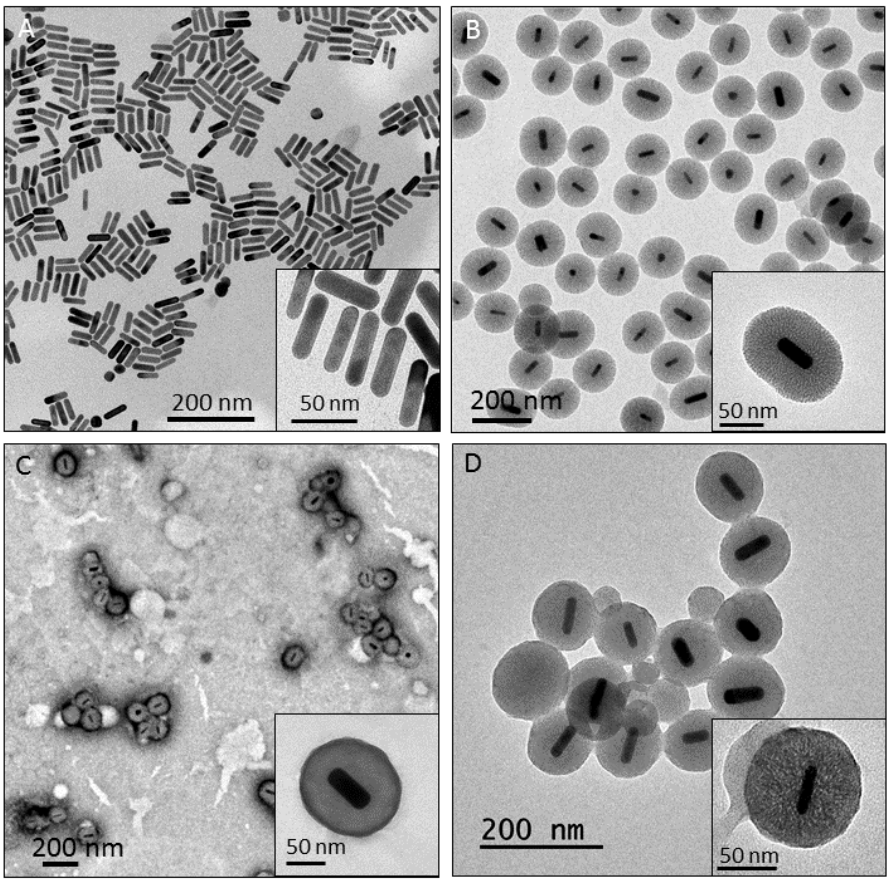

Figure 1: Representative transmission electron micrographs of GNR (**a**), GNR@MS (**b**) PR-NC (**c**) and PR-NC-NAP (**d**). The insets provide higher magnification images.

Mesoporous silica encapsulation (GNRs@MS) was carried out using a recently reported method based on a CTAB-templated sol-gel process that yielded mesoporous silica shells with radial pores (average diameter 2.1 nm) upon CTAB removal.[33] Representative TEM images of the silica coated GNRs are displayed in **Figure 1B** and in Figure S1 (Supporting Information), showing homogenous coating of individual GNRs, with no sign of aggregation. GNR@MS were then washed by centrifugation to remove small silica nanoparticles formed by TEOS condensation.

To avoid silica degradation in water,[44] the colloidal particles were re-dispersed in ethanol. Prior to the polymerization of pNIPAM/NHMA around the nanoparticles, it is necessary to introduce polymerizable groups onto the silica surface. For this purpose, and with the aim to functionalize only the nanoparticle surface, GNR@MS were treated with 3-[tris(trimethylsiloxy)silyl]propyl methacrylate (MPS) prior to surfactant extraction, following a reported method.[38] After this step, the CTAB template was removed by ionic exchange employing a solution of NH_4NO_3, to prevent the degradation of the new moiety (MPS). Once the particles are free of surfactant inside the silica channels, polymer coating was performed by radical polymerization, employing a monomer feed NIPAM/NHMA/MBA molar ratio of 0.85/0.10/0.05. This composition was established to obtain a lower critical solution temperature (LCST) at 42-43 ºC.[38] **Figure 1C** shows representative TEM images of PR-NC, where the polymer shell is observed as a dark coating around the particles, because phosphotungstic acid staining was applied to enhance the contrast of the organic shell.

Selectivity against melanoma cells was obtained by choosing the peptide NAPamide as the targeting moiety. NAPamide was thus synthetized with protected amine and acid groups within the main chain (**Scheme 2**).

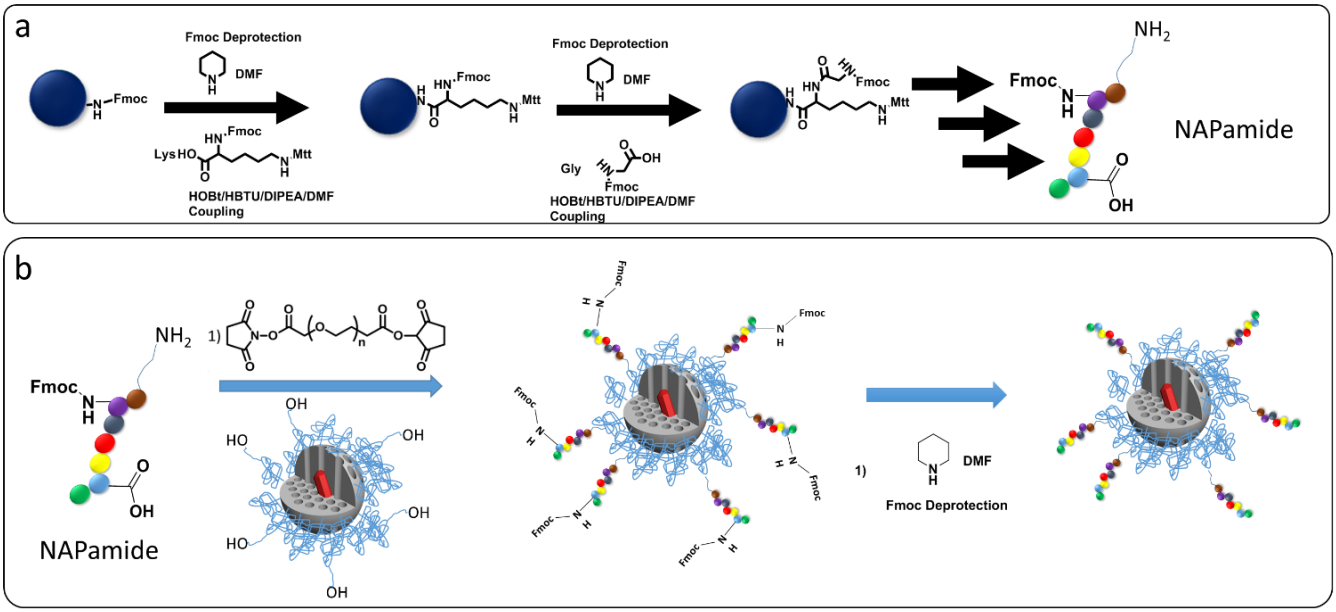

Scheme 2. a) Solid phase NAPamide synthesis, b) NAPamide PEGylation and coating over polymer surface on the PR-NC.

This methodology leaves only one amino nucleophilic active site localized in the lysine rest chain for the PEGylation process. The employed di-acid PEG ($(NHS)_2$PEG (2000 g/mol)) previously activated by NHS, enables the selective condensation of the free amino group with one of the acid groups of the PEG chain, even in the presence of the non-activated acid group from the aspartic acid in the initial peptide. Additionally, the absence of a base until the last step minimizes the aspartimide problem, which is very common in peptide sinthesys.[45] PEG/peptide condensation was carried out with a 1:1 ratio, preventing formation of the bis-adduct and leaving the acid group at the end of the PEG chain for subsequent *Steglich* esterification[46] with the available primary alcohol groups from the NHMA monomer in the polymer coating. Finally, an Fmoc deprotection step was carried out over the peptide-functionalized PR-NC, under mild conditions.

The nanoparticles were characterized by TEM, Z-potential, DLS, FTIR and TGA. FTIR was used to verify the successful functionalization of GNR@MS with MPS and further with the NIPAM/NHMA polymer, Figure S3. The spectra present a characteristic peak at 1100 cm^{-1} assigned to the Si–O vibration of silica. When the mesoporous silica nanoparticles were successfully functionalized with MPS, two characteristic peaks appeared at 1633 and 1702 cm^{-1} (C=O stretching). Upon deposition of the pNIPAM/NHMA polymer shell on the nanoparticles, these two peaks are hidden by three new bands due to the formation of a secondary amide (C=O stretching 1637 and 1532 cm^{-1}) and the deformation of methyl groups on $–C(CH_3)_2$ (1460 cm^{-1}), which is in accordance with previous pNIPAM/NHMA functionalizations.[38] Unfortunately, functionalization of the nanoparticles with NAPAmide did not lead to any variations in the FTIR spectra as expected, owing to the low amount that the targeting moiety represents as compared to the polymer bands, and the peptide bands being present within the same IR spectral region. Additionally, Z-potential measurements provided an estimate of the variation in surface charge during the functionalization process.

The Z-potential was found to vary from -14.4 mV for GNRs coated with silica (GNR@MS) to -21.6 mV when the polymer layer was grown on the surface. NAPamide anchoring on the polymer layer resulted in a very low surface charge (Z-Pot= -2.27 mV). TGA was also performed at all steps to confirm the successful functionalization of the nanoparticles and extraction of the surfactant. The final amount of polymer coating was determined as 36.45% of the total mass loss. (S.I. Figures S4 and S5.)

The amount of heat produced upon NIR irradiation depends on the NIR laser power and the concentration of nanoheaters, as well as on the irradiation time. It is well known that efficient hyperthermal therapy requires the local temperature to reach at least 43 ^{o}C,[17] at which protein denaturation and disruption of the cellular membrane would occur, leading to tumor tissue ablation. Studies at different particle concentrations were performed, from 10 μg/mL to 100 μg/mL. Different laser power densities were also tested to achieve the target temperature with the lowest possible power density, and to reduce residual side effects of NIR radiation. Additionally, exposure times of 5, 10 and 15 minutes were tested toward reaching the hyperthermia temperature in the shortest time possible. As described in **Table S2** of the Supporting Information, a hyperthermia macroscopic temperature required a concentration of nanoheaters of 50 μg/mL, 1 W/cm^2 NIR laser power density and 10 minutes of exposition time.

Drug loading and release capacities of the nanocarriers were tested using fluorescein as a model drug molecule. The mesoporous material PR-NC was incubated overnight under magnetic stirring at 50 ^{o}C in a saturated solution of fluorescein. The nanocarriers were then washed by centrifugation until the supernatant was clear, and subsequently dried in a vacuum oven at 30 ^{o}C. The fluorescein release experiments were performed by placing a dispersion of fluorescein-loaded nanocarriers (1 mg/mL) in a transwell permeable support in PBS. The different transwell plates were placed in two different ovens at 37 and 50 ^{o}C. An additional

transwell plate was placed in an oven at 37 ºC and irradiated with a NIR laser at 0.5 W/cm^2 for 10 minutes each hour. The PBS medium was measured by fluorescence spectroscopy and replaced every hour to estimate the amount of released fluorescein. As shown in **Figure 2**, fluorescein release was significantly enhanced under NIR laser irradiation, as compared to its counterpart in an incubator at 50 ^{0}C.

These results are in accordance with the existing literature,[38] where higher fluorescein release was achieved when heat was first produced at the nanoscale. In the case of magnetic hyperthermia, two effects have been described with PR-NC: (1) the collapse of the thermosensitive polymer structure leads to opening of the mesoporous silica pores, and (2) enhanced diffusion of fluorescein from the pores when the temperature was increased.[38] Although fluorescein leaking was observed at 37 ºC, it should be taken into consideration that the polymer coating acts as a diffusion barrier around the nanoparticle and fluorescein release is forced by the continuous replacement of the incubation media (PBS). Heating temperatures optimization of the material is shown on Table S2 in Supporting information.

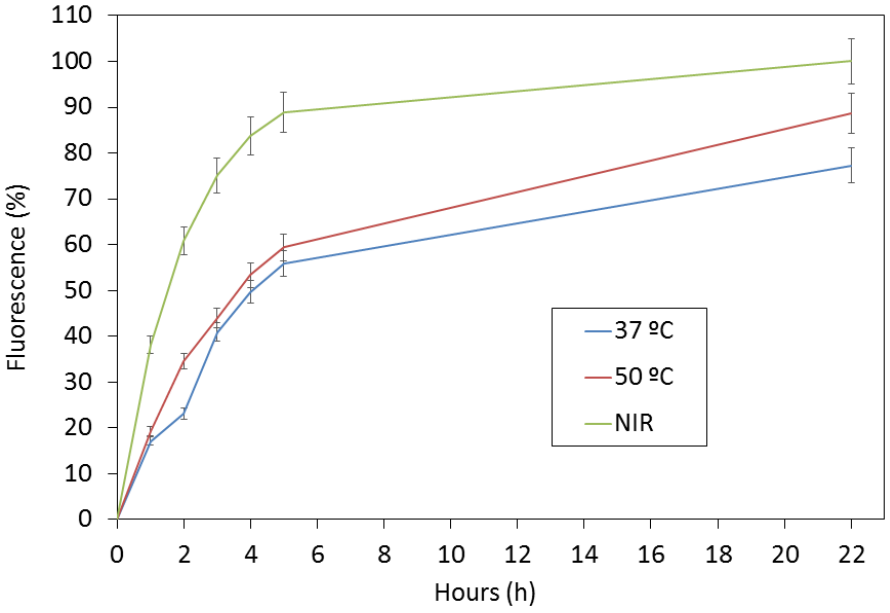

).

Figure 2: Responsive fluorescein release profile over time (24h) at 37 ºC and 50 ºC, and with NIR laser irradiation (1W, 10 min) for fluorescein loaded PR-NC.

In order to study the effect of the grafted NAPAmide targeting agent, FF_C108, a fibroblast healthy cell line from foreskin as control, and #17 melanoma cancer cells were seeded to carry out *in vitro* cellular uptake tests. Cell internalization was monitored by fluorescence microscopy (**Figure 3a**) and flow cytometry (**Figure 3b**), with tagged NCF-NAP and NCF. For this purpose, fluorescent mesoporous silica nanoparticles without metal cores were prepared as described in the experimental section.

For uptake experiments, a concentration of 75 µg/mL of NCF-NAP and NCF was used for both cell lines and both materials. The cell cultures were incubated for 24 hours and uptake was evaluated by flow cytometry measuring FITC percentage (**Figure 3b**), which represents the percentage of cells that had engulfed nanoparticles. **Figure 3a,b** shows that NCF nanoparticles did not internalize into either fibroblast or melanoma cells, which was expected due the negative surface charge of these nanoparticles. However, the presence of NAPAmide at the polymer surface promotes internalization of the NCF-NAP particles by both cell lines.

Our data clearly show that internalization in melanoma is higher (25%) than in the fibroblast healthy cell line, pointing toward a ligand–receptor mediated process besides the charge induction effect. As can be rationalized from the experiments, the uptake by melanoma cancer cells is higher than that for healthy cells, due to overexpression of NAPamide receptors on the melanoma cell wall.

In order to probe this differentiation in the internalization results from NAPamide interaction, a further experiment was performed to study cell uptake with different concentrations of NCF-NAP. **Figure 4** reveals that, in the best case (100 µg/mL), nanoparticle uptake by fibroblasts is almost 3 times lower than that by melanoma cancer cells. This difference however decreases when increasing the concentration of the targeted particles, due to receptor saturation, which allows us to conclude that the internalization process is concentration-dependent.

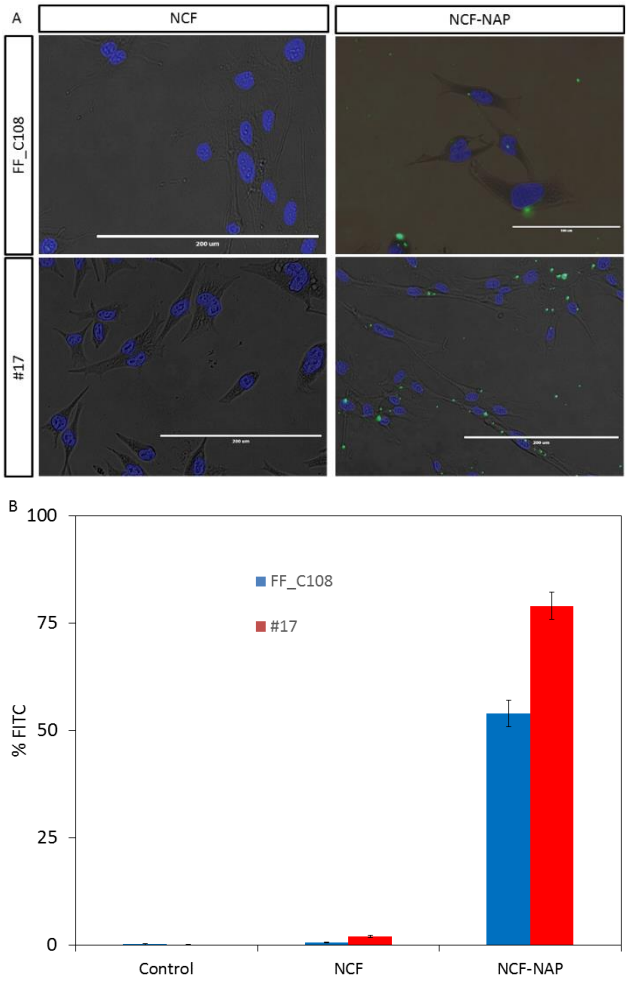

Figure 3: A) Optical microscopy images for both cell lines (#17 skin cancer cells and fibroblast FFC_C108) incubated with 75 µg/mL, for 2 hours, using NCF and NCF-NAP. Bar: 200 µm B) Cell uptake at 75 µg/mL, for 2 h, using NCF-NAP and NCF.

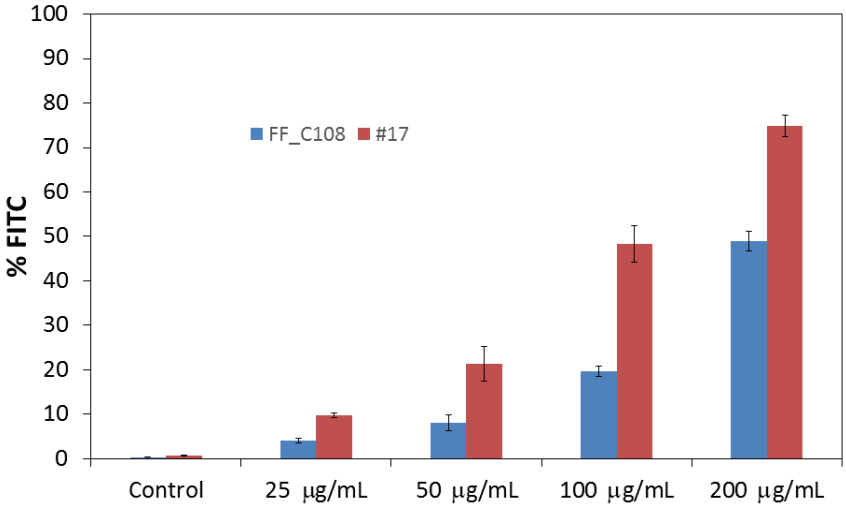

Figure 4: Dose-dependent cell uptake of NCF-NAP, for FF_C108, fibroblasts (control) and #17 melanoma cancer cells.

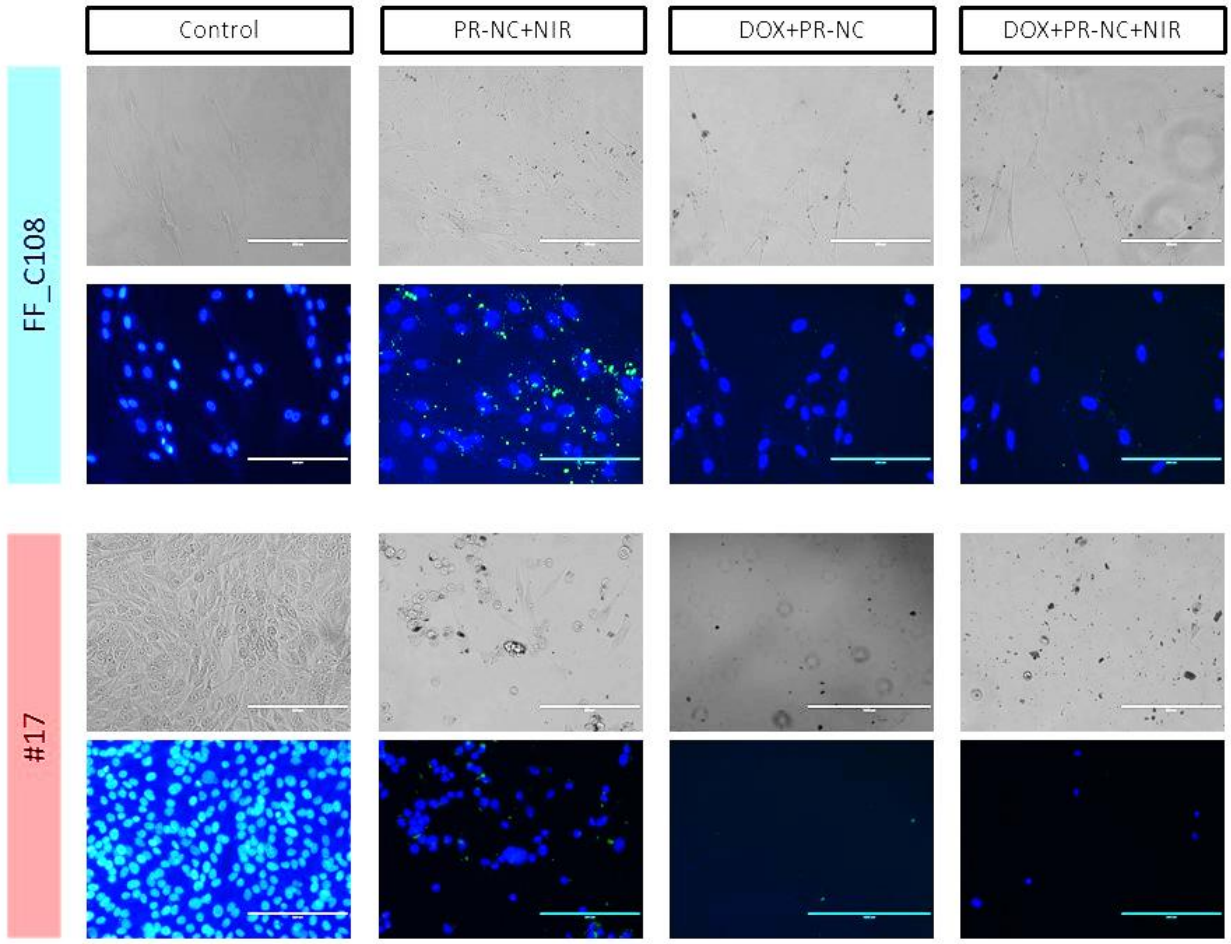

Figure 5. Optical microscopy images for cells incubated with 50 μg/mL of PR-NC-NAP and DOX-loaded PR-NC-NAP, with and without NIR irradiation. Bar 200 μm.

The final nanoparticle concentration in melanoma cancer cells appears to be higher than in fibroblasts at low concentrations, making more effective the potential synergy between chemo- and photo-thermal therapies, induced by the nanocarrier. To verify the synergistic effect of the treatment, the targeted nanocarrier was loaded with doxorubicin and tested in cell viability assays, as described in the experimental section. The same cell lines used for internalization experiments, i.e. FF_C108 (healthy fibroblast) and #17 (melanoma cancer cells), were employed, keeping in all experiments n=3. It is worth mentioning that nanoparticles and cells were incubated for 2 hours, and then the cells were washed with PBS twice to remove non-internalized nanoparticles. Cytotoxicity was tested using alamarBlue® assay, 24 hours after irradiation.

Figure 5 illustrates the cell viability of both cell lines treated with 50 μg/mL blank nanoparticles (free of DOX) and DOX-loaded nanoparticles. (For more information, see **Figure S10**) As expected, both cell lines maintain high viability values in the presence of unloaded nanocarriers, without NIR application. For melanoma cancer cells the viability decreases dramatically (up to 13%) when DOX- loaded nanoparticles are present in the culture medium. This effect can be attributed to the higher internalization of the nanoparticles in melanoma cancer cells and spontaneous DOX release. On the other hand, fibroblast cell viability was 72%, mainly due to lower nanocarrier uptake, added to the better defense mechanisms that healthy cells present against chemotherapeutics.[47] The same experiment groups (control, blank PR-NCF-NAP and DOX-loaded PR-NCF-NAP) with both cell lines, were irradiated with NIR light (808 nm, 1 W/cm^2) for 10 minutes, monitoring the temperature with a fluorooptic probe (this irradiation set up was fixed for every subsequent experiment). As can be observed, the viability controls were not affected by laser exposure. In the case of blank nanocarriers, a macroscopic temperature of 41 ^{0}C was reached after irradiation and a 55% decrease in cell viability was achieved only for melanoma cancer cells. Meanwhile, for fibroblasts cell viability was almost the same as for the nanoparticles control without NIR irradiation (77%).

We then studied the combined action of chemo and PPT effects, by incubating cells with DOX loaded PR-NCF-NAP and irradiating with the NIR laser. We found an extraordinary increase of cell death for melanoma cancer cells, down to 1% viability, whereas viability of the healthy cell line remains close to that of the DOX-loaded photoresponsive nanocarriers control (73%). These findings are again related to the enhanced nanocarrier uptake by melanoma cancer cells. Higher internalization rates lead to a higher concentration of both gold nanorods and drug inside the cells, resulting in a heat shock which effectively provokes cancer cell death by itself. In addition, the decrease in melanoma cell viability with the combined treatment (DOX+NIR laser) reveals that drug release is allowed through polymer

shrinkage, induced by the temperature rise inside living cells under NIR laser irradiation. On the other hand, it has been described in the literature that the cytotoxicity of DOX can be enhanced at higher temperature, thereby improving the cytotoxicity of the loaded drug.[48,49]

As discussed above, the thermosensitive polymer coating responds to temperature changes within the hyperthermia range. An additional important aspect about the heating mechanism should also be evaluated; namely, whether the temperature increment must be macroscopic in order to trigger the polymer transition or whether the local heating in close vicinity to the GNRs is sufficient to induce the polymer transition and pore opening. This "hot-spot" effect comprises a local heating when the gold nanorods are irradiated with a NIR laser, without reaching a macroscopic hyperthermia temperature. The presence of this effect in thermo-responsive materials allows the use of low nanoparticle doses because it is not necessary to increase the temperature all over the tissue to trigger drug release and subsequent cell death.

In order to test if the cytotoxic effect can be achieved without a macroscopic temperature rise, the concentration of nanoparticles was decreased by 5-fold and 10-fold, to prevent overall heating of the cell cultures. The macroscopic temperature after irradiation was monitored during the experiments, being ca. 38 ^{0}C in all cases. **Figure 6** shows the viability of both cell lines treated with low doses, (5 and 10 μg/mL) of blank and DOX-loaded PR-NC-NAP, as well as with and without NIR irradiation. As expected, both cell lines incubated with drug-free nanocarriers maintained a similar high viability as that of the controls without NIR irradiation. However, the cell viability of melanoma cancer cells exposed to 5 and 10 μg/mL significantly decreases (60 and 41%, respectively) when DOX-loaded PR-NC-NAP were used. On the contrary, the fibroblasts were only affected by the DOX-loaded nanoparticles at the higher dose (10 μg/mL). In the same cellular assay, both cell lines were irradiated with NIR light (808 nm), observing 15% melanoma cell viability at higher doses and almost no cell

death at the lower dose. It is also remarkable that the cell viability of fibroblasts is the same as that for non-irradiated cells exposed to the blank nanocarriers (100%).

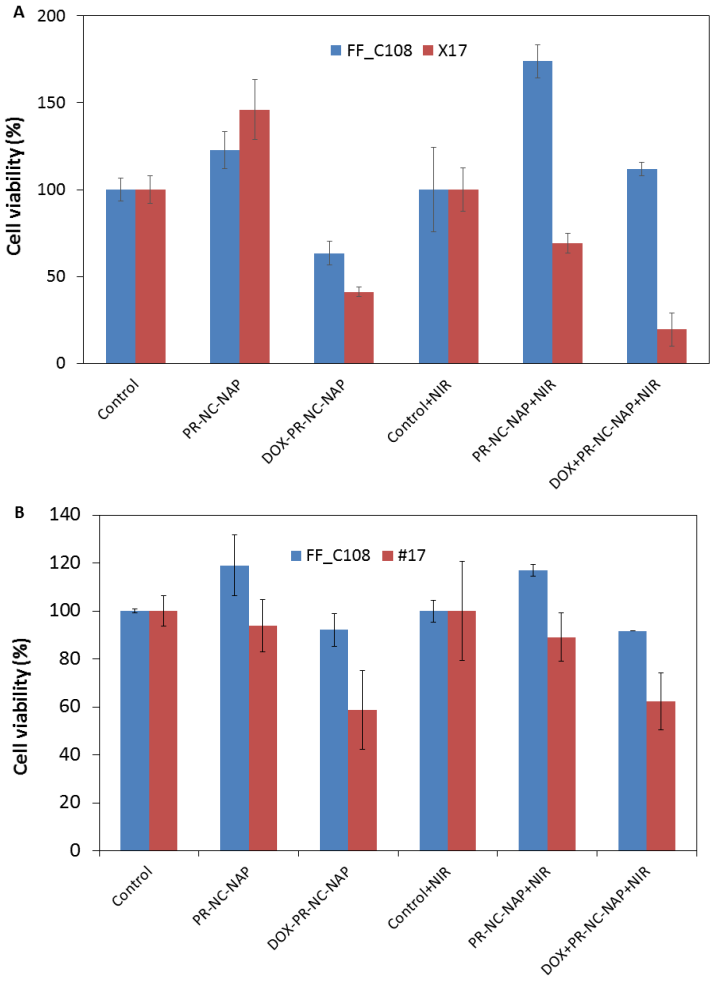

Figure 6: Cell viability at different nanocarrier concentrations, 10 μg/mL (A) and 5 μg/mL (B), for healthy fibroblasts and melanoma cancer cells.

When the melanoma cancer cells were incubated with DOX-loaded nanoparticles and irradiated with NIR laser, the viability of melanoma cells fell down to 24%, in the case of cells treated with 10 μg/mL, while at 5 μg/mL the viability decrease was less pronounced but still noticeable. This is a clear evidence of the synergistic effect of PTT and chemotherapy, at low nanoparticle dose. Again, the healthy fibroblasts were not affected by the DOX loaded nanocarriers treatment, even under NIR irradiation, at both concentrations. The treatment with DOX and NIR laser at low dose also shows that the viability of melanoma cells was the same, with or without laser irradiation. This could mean that the thermal effect is no longer enough

to overcome the cancer cell countermeasures. Even though the thermal effect is lost at very low concentrations, the chemotherapy treatment is still working, probably due to doxorubicin delivery mediated by NAPAmide targeting.

We finally explored the possibility to enhance cell death by multiple irradiations. Melanoma cancer cells were incubated as in previous assays, with 5 μg/mL of the final PR-NC-NAP (with and without DOX). Every 24h the cells were irradiated with NIR laser (808 nm) for 10 minutes at 1W/cm^2. Cell viability was evaluated by alamarBlue® assay, 24h after irradiation. As the viability assay is biocompatible, the culture medium of each sample was maintained during the test and replaced again at the end of the assay. As shown in **Figure S11**, cell viability was almost the same after 2 and 3 NIR-laser irradiations. This result is in agreement with the drug release experiment, where we found that after one irradiation almost half of the cargo was released, so a single NIR irradiation is sufficient to achieve the desired therapeutic effect.

3. Conclusion

In summary, multifunctional PR-NC-NAP composite nanoparticles were synthesized via radical polymerization onto GNR@MS hybrid nanoparticles. The nanoparticles demonstrated thermal/NIR laser sensitivity and outstanding photothermal conversion. The NAPamide peptide was demonstrated to be an excellent targeting ligand for melanoma cancer cells, as it could discriminate healthy cells of human fibroblast foreskin from metastatic ones. The viability of cancer cells treated with DOX-loaded nanocarriers was significantly reduced at relatively low nanoparticle concentration (10 μg/mL) and short NIR laser irradiation time (10 minutes). Thus, DOX-loaded nanoparticles exhibited high cytotoxicity as compared with chemotherapy or PTT alone, due to a synergistic effect between chemo and PTT, where NIR light acts as a trigger to induce DOX release from the nanoparticles through the temperature increase inside the cells, causing cell death. Our results demonstrate the feasibility of such nanocarriers to be a powerful instrument for drug delivery systems, in response to

thermal/NIR laser irradiation, for melanoma cancer cells, on account of the discrimination between cancerous and healthy cells present in tumors. Our nanocarriers could be exploited as a combined chemo-PTT system, with improved therapeutic efficacy even at low drug dose for superficial tumors, being a promising candidate for "in vivo" evaluation.

4. Experimental Section

Materials

Amino-protected Fmoc aminoacids, piperidine, N,N,N′,N′-Tetramethyl-O-(1H-benzotriazol-1-yl)uronium hexafluorophosphate, O-(Benzotriazol-1-yl)-N,N,N′,N′-tetramethyluronium hexafluorophosphate (HBTU), 1-Hydroxybenzotriazole hydrate (HOBT), Diisopropyl Ethyl amine (DIPEA), Trifluoroacetic acid (TFA), Triisopropyl silane (TIPS), O,O′-Bis[2-(N-Succinimidyl-succinylamino)ethyl]polyethylene glycol 2KDa, Rink amide resin, Sephadex G-25, as well as the solvents used in the condensation, deprotection and release stages, such as N',N'-dimethylformamide (DMF) and dichloromethane (DCM), gold chloride trihydrate ($HAuCl_4.3H_2O$), ammonium nitrate ($NaNO_3$), Sodium carbonate (Na_2CO_3), cetyltrimethylammonium bromide (CTAB), tetraethyl orthosilicate (TEOS), amminopropyltriethoxysilane (APTES), 3-(trimethoxysilyl)propyl methacrylate (MPS), as well as the reagents for polymerization, N-isopropylacrylamide (NIPAM,≥99%), N-(hydroxymethyl)acrylamide solution (NHMA, 48 wt % in H2O), N,N′-methylenebis(acrylamide) (MBA, 99%), ammonium persulfate (APS), and fluorescein sodium salt were also purchased from Sigma-Aldrich.

All other chemicals (absolute ethanol, acetone, ethyl acetate, heptane, dry solvents, ammonium nitrate, etc.) were of the highest commercially available quality and used as received.

GNR@MS: GNRs were prepared using a modified seeded growth method.[50] Gold concentration was determined from the extinction spectra using the absorbance at 400 nm.[51]

Coating of Au NRs with mesoporous silica was performed following a previously described protocol,[33] with minor modifications. Excess reactants were removed from the freshly prepared GNR solutions via two cycles of centrifugation, after which the particles were resuspended in 0.1 M CTAB, at a final gold concentration of 5 mM. Subsequently, 20.4 mL of a 6 mM CTAB solution was mixed with 60 mL of ethanol and 134 mL of water at 30 ºC in a 500 mL round beaker under magnetic stirring. Upon equilibration at 30 °C for 10 min, 400 μL of NH_4OH (25 vol %) was added to adjust the pH value to ca. 9. Then, 6 mL of the GNR solution was poured into the synthesis solution. After 5 min to ensure homogeneity of the solution, 160 μL of TEOS was added dropwise under vigorous stirring. The reaction mixture was allowed to react at 60 °C for two days. The synthesized particles were centrifuged (30 min; 7500 rpm; 35 °C), and washed in ethanol.

Fluorescein-labeled GNR@MS (GNR@MSF): GNR@MSF were synthesized using the same procedure, except that APTES-FITC (25 μL) was added at low temperature (30 °C) after 5 hours of silica growth and the temperature was then set again to 60 °C for the remaining reaction time (two days).

Nanoparticles (GNR@MS, GNR@MSF, MSNF) coated with pNIPAM/NHMA (PR-NC, PR-NCF and NCF respectively): Once GNR@MS were synthetized, the polymer layer was formed as described by Baeza and coworkers.[37] 40 mL of *GNR@MS*, GNR@MSF or MSNF (1.5 mg/mL) were poured in a 100 mL round-bottom flask and 0.4 mL of MPS was added in order to functionalize the surface with methacrylate groups where the further polymerization will take place (GNR@MS@MPS, GNR@MSF@MPS or MSNF@MPS). After magnetic stirring for 12 h at 40 ºC, the mixture was washed twice by centrifugation and redispersed in ethanol. The surfactant template was removed by ion exchange, using an extracting solution comprising 1.59 g of NH_4NO_3, 573 mL of EtOH (99.6 %) and 27 mL of water. The mixture was heated up to 70 ºC and stirred overnight. Then, the solution was washed twice by centrifugation and redispersied in ethanol. Upon surfactant extraction, polymer coating was

carried out following a well described protocol.[38,52] In a 100 mL three-neck round bottom flask, 142.5 mg (1.33 mmol) of NIPAM, 12 mg of MBA (0.078 mmol), 33.1 μL of NHMA (0.148 mmol), 3.6 mg of CTAB, and 5 mg of Na_2CO_3 were added to 45 mL of water. The solution was stirred under N_2 bubbling at 70 °C for 30 min to remove oxygen. Meanwhile, the solution of NIPAM/NHMA was kept under N_2, 50 mg of MPS functionalized nanocarrier was redispersed in 5 mL of Ethanol (99.5%) and kept under N_2 bubbling for 20 min to remove oxygen. Then, 5 mL of MPS functionalized nanocarrier was added to the monomer solution and magnetically stirred for 15 min to homogenize. To initiate the monomer polymerization, 0.2 mL of a 25 mg/mL APS solution in previously deoxygenated H_2O (mQ) was added to the reaction mixture. Ten minutes after addition of the initiator, the reaction mixture was allowed to cool down to room temperature for 12 h. The mixture was centrifuged and washed twice with THF to remove unreacted monomers, twice with ethanol and again twice with water. Finally, it was dried under vacuum overnight.

Mesoporous silica labeled with fluorescein (MSNF): Fluorescent Mesoporous Silica Nanoparticles (MSNF), were synthesized by a modified Stöber method, from TEOS in the presence of CTAB as a structure directing agent. Fluorescein-labeled nanoparticles were synthesized by mixing 1 mg of fluorescein isothiocyanate with 2.2 μL APTES in 50 μL ethanol for 2h. Then the reaction mixture was mixed with 5 mL of TEOS. In a round-bottom flask, 1 g of CTAB, 480 mL of H_2O (Milli-Q) and 3.5 mL of NaOH (2 M) were added. The mixture was heated to 80 °C and gently stirred. Then, 5 mL of TEOS mixed with 52.2 μL of the APTES-fluorescein product were added dropwise at 0.25 mL/min rate, with a pump. After two hours, the reaction mixture was centrifuged and washed with water and ethanol. (For more information about nanoparticles synthesis and functionalization, see Supporting Information Scheme S1 and Figures S1-S5)

NAPamide Targeting Agent Synthesis: NAPamide synthesis was carried out through a conventional solid phase Fmoc/coupling methodology, previously used in our group.[53] Fmoc

protected amino acids were condensed to each other following the sequence Fmoc-NH-Nle-Asp-His-D,Phe-Arg-Trp-Gly-Lys-$CONH_2$. In this case, we used Rink amide resin to obtain an amide group in the acid final position, and Fmoc protected extreme amine. This analogue would be ready for the PEGylation step, prior to anchoring to the nanoparticle NIPAM/NHMA co-polymer.

The starting Rink amide resin (1 mmol NH-Fmoc/gr x 0.3 gr) was activated by suspension in a DMF/piperidine 20% solution for primary amine Fmoc deprotection. After washing steps with DMF, the first aminoacid, (NHMtt)LysFmoc (3Eq) was condensed to the resin through a HBTU/HOBT/DIPEA (3Eq/3Eq/6Eq) typical coupling reaction and all the amino acids were deprotected and coupled until the end group, which was not unprotected. The final cleavage step was performed by incubation of the resin in a cocktail mixture of TFA/TIPS/H_2O (95/2.5/2.5). The crude was afforded by precipitation of the filtered solution in cold ethyl ether, which was purified by flash column for molecular exclusion chromatography (stationary phase: Sephadex® G-25; mobile phase: water). Around 30 mg of isolated peptide was frozen at -80 °C and lyophilized prior to characterization (For more information about NAPamide synthesis, see Supporting Information Scheme S2 and Figures S6-S9).

Targeting agent anchoring of PR-NC, PR-NCF and NCF*:* To a solution of $(NHS)_2$PEG (2000 g/mol) (11 mg, 1 mL DMF), Fmoc-protected NAPamine was added drop-wise (7 mg in 1 mL of DMF and 10 µL of TEA) under inert atmosphere. When the addition was finished, the reaction mixture was stirred overnight. The mixture was added dropwise to each nanocarrier previously obtained, PR-NC, PR-NCF and NCF, (12 mg) dispersion in DCM under nitrogen flow and the new mixture was stirred overnight. The functionalized nanoparticles were isolated and purified by successive washings with DCM, ethanol and water. Finally, Fmoc deprotection was carried out with 2mL of DMF/Piperidine solution (20%). The material was dried under vacuum and characterized. (See Supporting information Scheme S3)

Drug loading: All synthetized materials were loaded with doxorubicin hydrochloride by suspension of 2 mg of each material in 1 mL of ca. 5 mg/mL DOX solution in PBS. The suspension was stirred at 50 ºC for 24 h and the nanomaterials were thoroughly washed with H_2O 5-fold, until the typical red color from DOX disappeared from the solution.

Internalization assay: #17 (melanoma skin cancer cells) and FF_C108 (fibroblast foreskin cells) were seeded in Dulbecco's modified eagle medium (DMEM) and incubated in 24-well plates at 40,000 cells/well, for 24 hours at 37 ºC, 5% CO_2 and 95% humidity. Cells were exposed to several concentrations of fluorescein tagged nanocarriers, for 2 hours under incubation conditions.

Cells were then washed with PBS and incubated again in DMEM at the same conditions for 24 hours. After the uptake time ended, the cells were washed again with PBS, harvested and treated with trypan blue. The percentage of FITC+ cells and mean fluorescence indexes (MFI) were obtained by flow cytometry using a FACSCanto II flow cytometer and the FACSDiva software v6.1.2 (BD Biosciences, San Jose, Ca.).

Cytotoxicity in vitro assays: In order to evaluate the cytotoxicity of doxorubicin hydrochloride loaded on PR-NC-NAP *in vitro,* #17 (melanoma skin cancer cells) and FF_C108 (fibroblast foreskin cells) were seeded in 24-well plates at 40,000 cells/well, at 37 ^{0}C, 5% CO_2 and 95% humidity, in DMEM. Cells were exposed to different concentrations of the loaded targeted nanocarrier for 2 hours and then washed with PBS to place them atincubation conditions again. Cell viability was determined by alamarblue® assay at various times. Percentages of dead cell populations are shown as the normalized mean of three independent replicates.

Characterization

UV-visible spectra were obtained using a HELIOS-ZETA UV-vis spectrophotometer. Transmission electron microscopy (TEM) images were obtained in a JEOL 1400 transmission electron microscope (TEM). The p-NIPAM/NHMA coating and the polymer plus targeting

samples were observed after staining the organic layer with 1% phosphotungstic acid. The hydrodynamic size of mesoporous nanoparticles was measured by means of a Zetasizer Nano ZS (Malvern Instruments) equipped with a 633 nm laser. Zeta potential was measured by a Zetasizer Nano ZS (Malvern Instruments). All measurements were performed in triplicate. FTIR spectra were measured on a Nexus spectrometer equipped with a Goldengate attenuated total reflectance device. Thermogravimetric analysis was performed in a Perkin Elmer Pyris Diamond TG/DTA analyzer, with 5 ^{o}C/min heating ramps, from room temperature to 600 ^{o}C. Liquid NMR experiments were made in a Bruker AV 250MHz. Mass spectra were acquired with a Voyager DE-STR Biospectrometry MALDI-TOF mass spectrometer. A Newport Diode Laser was used, with a continuous-wave NIR laser at 808 nm, the maximum fluence was 3 W/cm2 and the spot size 5 mm. Pre- and post-illumination temperatures of the control experiments were measured by a fluorooptic probe Luxtron I652.

Abbreviations

Mtt……protecting group methyltrityl, typical for primary amine.

Acronyms for materials names :

1– GNR@MS@NIPAM ---------- PR-NC

2– GNR@MS@NIPAM@NAPamide----- PR-NC-NAP

3– GNR@MSF@NIPAM ---------- PR-NCF

4– GNR@MSF@NIPAM@NAPamide---- PR-NCF-NAP

5– MSNF@MS@NIPAM ---------- NCF

6– MSNF@MS@NIPAM@NAPamide---- NCF-NAP

PR: Photoresponsive

NC: Nanocarrier

NAPA: Napamide, targeting

NCF: Fluorescent Nanocarrier

Supporting Information
Supporting Information is available from the Wiley Online Library or from the author.

Acknowledgements
This work was supported by the European Research Council (Advanced Grant VERDI; ERC-2015-AdG No. 694160) and the MINECO grants MAT2015-64831-R and MAT2017-86659-R. SGG acknowledges the Juan de la Cierva – Formación 2014 program (FJCI-2014-2016). Acknowledgements to Prof. María S. Soengas for providing the study cell lines. C.H. acknowledges the Alexander von Humboldt Foundation for funding through a Feodor Lynen Fellowship.

Received: ((will be filled in by the editorial staff))
Revised: ((will be filled in by the editorial staff))
Published online: ((will be filled in by the editorial staff))

References

[1] G. Merlino, M. Herlyn, D. E. Fisher, B. C. Bastian, K. T. Flaherty, M. A. Davies, J. A. Wargo, C. Curiel-Lewandrowski, M. J. Weber, S. A. Leachman, M. S. Soengas, M. McMahon, J. W. Harbour, S. M. Swetter, A. E. Aplin, M. B. Atkins, M. W. Bosenberg, R. Dummer, J. E. Gershenwald, A. C. Halpern, D. Herlyn, G. C. Karakousis, J. M. Kirkwood, M. Krauthammer, R. S. Lo, G. V. Long, G. McArthur, A. Ribas, L. Schuchter, J. A. Sosman, K. S. Smalley, P. Steeg, N. E. Thomas, H. Tsao, T. Tueting, A. Weeraratna, G. Xu, R. Lomax, A. Martin, S. Silverstein, T. Turnham, Z. A. Ronai, *Pigment Cell Melanoma Res.* **2016**, *29*, 404.

[2] V. Gray-Schopfer, C. Wellbrock, R. Marais, *Nature* **2007**, *445*, 851.

[3] M. R. Wick, *Semin. Diagn. Pathol.* **2016**, *33*, 225.

[4] T. Quinn, X. Zhang, Y. Miao, *G. Ital. di dermatologia e Venereol. organo Uff. Soc. Ital. di dermatologia e Sifilogr.* **2010**, *145*, 245.

[5] G. Ren, S. Liu, H. Liu, Z. Miao, Z. Cheng, *Bioconjug. Chem.* **2010**, *21*, 2355.

[6] J. P. Bapst, A. N. Eberle, *Front. Endocrinol. (Lausanne).* **2017**, *8*, 1.

[7] M. H. and B. C. B. Edward R. Sauter, Un-Cheol Yeo, Andrea von Stemm, Weizhu Zhu, Samuel Litwin, David S. Tichansky, Giuseppa Pistritto, Mark Nesbit, Dan Pinkel, **2002**, 79.

[8] A. M. Elliott, M. Al-Hajj, *Mol. cancer Res.* **2009**, *7*, 79.

[9] M. S. Soengas, S. W. Lowe, *Oncogene* **2003**, *22*, 3138.

[10] S. Hosemann, *OncoLog* **2011**, *56*.

[11] Y. Zhao, S. Tang, J. Guo, M. Alahdal, S. Cao, Z. Yang, F. Zhang, Y. Shen, M. Sun, R. Mo, L. Zong, L. Jin, *Sci. Rep.* **2017**, *7*, 1.

[12] X. Zhang, J. G. Teodoro, J. L. Nadeau, *Nanomedicine Nanotechnology, Biol. Med.* **2015**, *11*, 1365.

[13] H. Maeda, H. Nakamura, J. Fang, *Adv. Drug Deliv. Rev.* **2013**, *65*, 71.

[14] J. Fang, H. Nakamura, H. Maeda, *Adv. Drug Deliv. Rev.* **2011**, *63*, 136.

[15] H. Nakamura, F. Jun, H. Maeda, **2015**, 53.

[16] A. M. Mansour, J. Drevs, N. Esser, F. M. Hamada, O. A. Badary, C. Unger, I. Fichtner, F. Kratz, *Cancer Res.* **2003**, *63*, 4062.

[17] X. Huang, I. H. El-Sayed, W. Qian, M. A. El-Sayed, *J. Am. Chem. Soc.* **2006**, 128, 6.

[18] H. Tang, S. Shen, J. Guo, B. Chang, X. Jiang, W. Yang, *J. Mater. Chem.* **2012**, *22*, 16095.

[19] R. Zhao, X. Han, Y. Li, H. Wang, T. Ji, Y. Zhao, G. Nie, *ACS Nano*, **2017,** *11*, 8.

[20] Y. Li, T. Wen, R. Zhao, X. Liu, T. Ji, H. Wang, X. Shi, J. Shi, J. Wei, Y. Zhao, X. Wu, G. Nie, *ACS Nano***, 2014,** *8*, 11, 11529.

[21] H. C. Huang, K. Rege, J. J. Heys Ḱ, *ACS Nano***, 2010,** 4, 5, 2892.

[22] J. S. Donner, S. A. Thompson, M. P. Kreuzer, G. Baffou, R. Quidant, *Nano Lett.*, 2012, *12*, 4, 2107.

[23] R. Weissleder, *Nat. Biotechnol.* **2001**, *19*, 316.

[24] Y. Wang, Kvar, C. L. Black, H. Luehmann, W. Li, Y. Zhang, X. Cai, D. Wan, S. Y. Liu, M. Li, P. Kim, Z.-Y. Li, L. V Wang, Y. Liu, Y. Xia, *ACS Nano*, 2013, *7*, 3, 2068.

[25] K. Yang, S. Zhang, G. Zhang, X. Sun, S. T. Lee, Z. Liu, *Nano Lett.*, 2010, *10*, 9, 3318.

[26] H. K. Moon, S. H. Lee, H. C. Choi, *ACS Nano*, 2009, *3*, 11, 3707.

[27] S. C. Nguyen, Q. Zhang, K. Manthiram, X. Ye, J. P. Lomont, C. B. Harris, H. Weller, A. Paul Alivisatos, *ACS Nano*, 2016, 10, 2, 2144.

[28] *J. Photochem. Photobiol. B Biol.* **2000**, *57*, 90.

[29] R. Tong, D. S. Kohane, *Annu. Rev. Pharmacol. Toxicol.* **2016**, *56*, 41.

[30] X. Huang, P. K. Jain, I. H. El-Sayed, M. A. El-Sayed, *Lasers Med. Sci.* **2008**, *23*, 217.

[31] J. Pérez-Juste, I. Pastoriza-Santos, L. M. Liz-Marzán, P. Mulvaney, *Coord. Chem. Rev.* **2005**, *249*, 1870.

[32] T. Niidome, M. Yamagata, Y. Okamoto, Y. Akiyama, H. Takahashi, T. Kawano, Y. Katayama, Y. Niidome, *J. Control. Release* **2006**, *114*, 343.

[33] M. N. Sanz-Ortiz, K. Sentosun, S. Bals, L. M. Liz-Marzán, *ACS Nano* **2015**, *9*, 10489.

[34] S. Shen, H. Tang, X. Zhang, J. Ren, Z. Pang, D. Wang, H. Gao, Y. Qian, X. Jiang, W. Yang, *Biomaterials* **2013**, *34*, 3150.

[35] M. Vallet-Regi, A. Rámila, R. P. del Real, J. Pérez-Pariente, *Chem. Mater.* **2001**, *13*, 308.

[36] M. Vallet-Regí, F. Balas, D. Arcos, *Angew. Chem. Int. Ed. Engl.* **2007**, *46*, 7548.

[37] A. Baeza, E. Guisasola, E. Ruiz-Hernandez, M. Vallet-Regi, *Chem. Mater.* **2012**, *24*, 517.

[38] E. Guisasola, A. Baeza, M. Talelli, D. Arcos, M. Moros, J. M. De La Fuente, M. Vallet-Regí, *Langmuir* **2015**, *31*, 12777.

[39] Y. Wang, K. Wang, J. Zhao, X. Liu, J. Bu, X. Yan, R. Huang, *J. Am. Chem. Soc.* 2013, 135, *12*, 4799.

[40] Z. Song, J. Shi, Z. Zhang, Z. Qi, S. Han, S. Cao, *J. Mater. Sci.* **2018**, *53*, 7165.

[41] S. Baek, R. K. Singh, T. H. Kim, J. W. Seo, U. S. Shin, W. Chrzanowski, H. W. Kim, *ACS Appl. Mater. Interfaces* **2016**, *8*, 8967.

[42] D. T. Marquez, J. C. Scaiano, *Langmuir* **2016**, *32*, 13764.

[43] J. Lee, C. Jeong, W. J. Kim, *J. Mater. Chem. B* **2014**, *2*, 8338.

[44] J. L. Paris, M. Colilla, I. Izquierdo-Barba, M. Manzano, M. Vallet-Regí, *J. Mater. Sci.* **2017**, *52*, 8761.

[45] M. Mergler, F. Dick, *J. Pept. Sci.* **2005**, *11*, 650.

[46] B. Neises, W. Steglich, Angewante Chemie, **1978**, 522.

[47] G. Housman, S. Byler, S. Heerboth, K. Lapinska, M. Longacre, N. Snyder, S. Sarkar, *Cancers (Basel).* **2014**, *6*, 1769.

[48] W. Zhang, Z. Guo, D. Huang, Z. Liu, X. Guo, H. Zhong, *Biomaterials* **2011**, *32*, 8555.

[49] S. Kossatz, J. Grandke, P. Couleaud, A. Latorre, A. Aires, K. Crosbie-Staunton, R. Ludwig, H. Dähring, V. Ettelt, A. Lazaro-Carrillo, M. Calero, M. Sader, J. Courty, Y. Volkov, A. Prina-Mello, A. Villanueva, Á. Somoza, A. L. Cortajarena, R. Miranda, I. Hilger, *Breast Cancer Res.* **2015**, *17*, 66.

[50] L. Scarabelli, M. Grzelczak, L. M. Liz-Marzán, *Chem. Mater.* **2013**, *25*, 4232.

[51] L. Scarabelli, A. Sánchez-Iglesias, J. Pérez-Juste, L. M. Liz-Marzán, *J. Phys. Chem. Let.* **2015**, *6*, 4270.

[52] A. Baeza, E. Guisasola, A. Torres-Pardo, J. M. González-Calbet, G. J. Melen, M. Ramirez, M. Vallet-Regí, *Adv. Funct. Mater.* **2014**, *24*, 4625.

[53] G. Villaverde, V. Nairi, A. Baeza, M. Vallet-Regí, *Chem. A Eur. J.* **2017**, *23*, 30.

Core-multishell gold nanorods, coated with mesoporous silica and further covered with a thermosensitive polymer were vectorized for selective internalization in melanoma cells. The proposed nanoformulation is capable of releasing the transported cytotoxic compounds on demand, in response to near-IR irradiation, with high selectivity and efficacy against malignant cells, even at low concentrations, thereby providing a new tool against melanoma disease.

Keyword NAPamide, melanoma, photothermal therapy

Gonzalo Villaverde,[a#] Sergio Gómez-Graña,[a#] Eduardo Guisasola,[a] Isabel García,[b] Christoph Hanske,[b] Luis M. Liz-Marzán,[b,c] Alejandro Baeza,[a,*] Maria Vallet-Regí[a]

Targeted Chemo-Photo Thermal Therapy: a Nanomedicine Approximation to Selective Melanoma Treatment.